



# Rapid design of corner restraining force in deep drawn rectangular parts

Hong Yao, Brad L. Kinsey, Jian Cao \*

*Department of Mechanical Engineering, Northwestern University, Evanston, IL 60208, USA*

Received 20 November 1998; accepted 21 April 1999

---

## Abstract

With the development of finite element method and computer technology, the complete modeling of the forming of a 3D sheet metal part is becoming realistic. However, an accurate 3D simulation is usually too time-consuming to be used in the early stage of design. One solution is to model the straight side of a 3D part as a plane strain problem and the corner section as an axisymmetric problem. Unfortunately, the axisymmetric solution often over-predicts the severity of the deformation at the corner and leads to a very conservative design. In this study, a modified axisymmetric model with a center offset is proposed to predict tearing failure in the corner sections of 3D parts. The proposed offset is found to be a function of the center strains, failure height, and tooling/process parameters, including tooling geometry, material properties, friction coefficient, and restraining force provided by the binder. Finite element analyses of both 3D and 2D axisymmetric models for square and rectangular cup forming are utilized to verify the proposed concept and to define the function. Excellent predictions of the failure heights are obtained. The proposed model enables engineers to rapidly specify the right amount of the restraining force in the corner section based on the desired center strains and forming depth. A detailed design algorithm is provided. © 1999 Elsevier Science Ltd. All rights reserved.

*Keywords:* Sheet metal forming; Failure prediction; Axisymmetric model; Tooling design; Process design

---

## 1. Introduction

The competitive global market pressures industries to shorten their development cycles and to reduce manufacturing costs. One solution would be to have reliable simulation models to aid product and process design during the early stages of development. As a key process in the

---

\* Corresponding author. Tel.: +1-847-467-1032; fax: +1-847-491-3915.  
*E-mail address:* jcao@nwu.edu (J. Cao)

automobile industry, extreme efforts have been made to numerically simulate sheet metal forming processes using the Finite Element Method (FEM). However, in many cases, the setup and computation time for the complete modeling of a 3D part forming is still too long to make simulations effective in assisting the design process. Therefore, simplified 2D models, which can predict forming processes reasonably well, are in great demand.

The methodology of using a simplified model was explored in Doege [1] where the factors affecting the formability were examined. In his analysis, an equivalent punch diameter was found for rectangular or irregular parts by calculating a circular punch of equal cross sectional area. In other words, an axisymmetric cup with an equivalent (fictitious) diameter was used to predict the limiting draw ratio of the rectangular or irregular cup. The clearances between the die and the punch were the same in the 3D and 2D models. The binder force used in the 2D model was calculated based on the material strength and tooling geometry. The draw ratio in his paper was defined as the ratio of blank diameter to punch diameter. The limiting draw ratio based on the equivalent cylinder cup was found to be lower than that of the rectangular part obtained in industrial stampings. The author attributed the inconsistency to the use of draw beads to increase the restraining force in the straight sides compared to the corner area in a rectangular part forming.

Saran et al. [2] analyzed the forming of complex parts with irregular tooling shapes using section analysis. In each section, a plane strain condition was assumed. The analysis can successfully simulate the deformation of many local sections where the strain states are close to plane strain. Brooks et al. [3] also demonstrated the application of 2D models in the design of a sheet metal forming process. A plane strain or axisymmetric assumption was made along a critical section of the die. Since these 2D models provided quantitative and qualitative information for the die design, they helped to eliminate the time intensive die try out method. Walker et al. [4] suggested that axisymmetric cup analysis could provide approximate, though conservative, solutions for near axisymmetric conditions, where the circumferential stress gradient is small.

Wong et al. [5] studied the corner design in deep drawn rectangular parts. They pointed out that axisymmetric cup analysis was not adequate to solve the corner deep drawing of rectangular parts. In the square cup forming process, the sheet metal originally in the straight section flows to the corner while it is drawn into the die cavity assisting the deep drawing in the corner region. If the corner part is treated as an axisymmetric cup, the predicted failure height is much lower than the experimental data. Several attempts were made to modify the axisymmetric boundary conditions such as changing the restraining force and blank size to promote material draw-in. The results were improved somewhat, but punch failure heights did not reach the level found in an actual 3D forming.

From the above review and practice in industry, simplified section analysis assuming a plane strain condition has been proven successful in designing the straight sections of stampings. However, the axisymmetric solution for the corners of the parts over-predicts the severity of the deformation and provides a very conservative design. In Section 2 of this paper, we propose a simplified 2D axisymmetric model with a center offset to predict tearing failure in the corner sections of complicated 3D parts. Section 3 serves the purpose of calibrating our numerical model so that results obtained from the following numerical analysis are reliable. To achieve this, deep-drawing experiments of a square cup were conducted. Using the  $FLD_0$  as a failure criterion, excellent agreement in failure heights between numerical and experimental results was achieved. The method of finding the correct center offset is illustrated in Section 4. Section 5 discusses the

effect of tooling/process parameters on the center offset. Through numerical simulations of square and rectangular cup drawing, the offset is found to be a function of center strains, forming depth, and the tooling/process parameters. Finally, in Section 6, a design algorithm is formulated to obtain the binder force required for a desired center strain and forming depth.

## 2. Axisymmetric model with a center offset

This work aims to provide a methodology for building a simplified 2D axisymmetric model for predicting the tearing failure height in a corner section of a complicated 3D part. We will start with rectangular cup forming to establish the key elements in this simplified approach and will generalize the relationship in upcoming research.

Fig. 1 shows the plan view of a quarter of a rectangular cup and simplified 2D models.  $B_1$ ,  $B_2$  and  $P_1$ ,  $P_2$  are half of the blank and punch sizes respectively,  $c$  is the clearance between the punch and the die, and  $b_1$ ,  $b_2$  are the length of the blank under the binder in the two directions. The subscripts 1, 2 denote the dimensions in the  $x$  and  $y$  direction, respectively. Region OABD is considered as the corner of the part, and point C is the center of the rectangular cup. The conventional method treats the corner part (OABD) as an axisymmetric cup and uses OEF as the simplified 2D axisymmetric model. As a result the model does not take into account the material

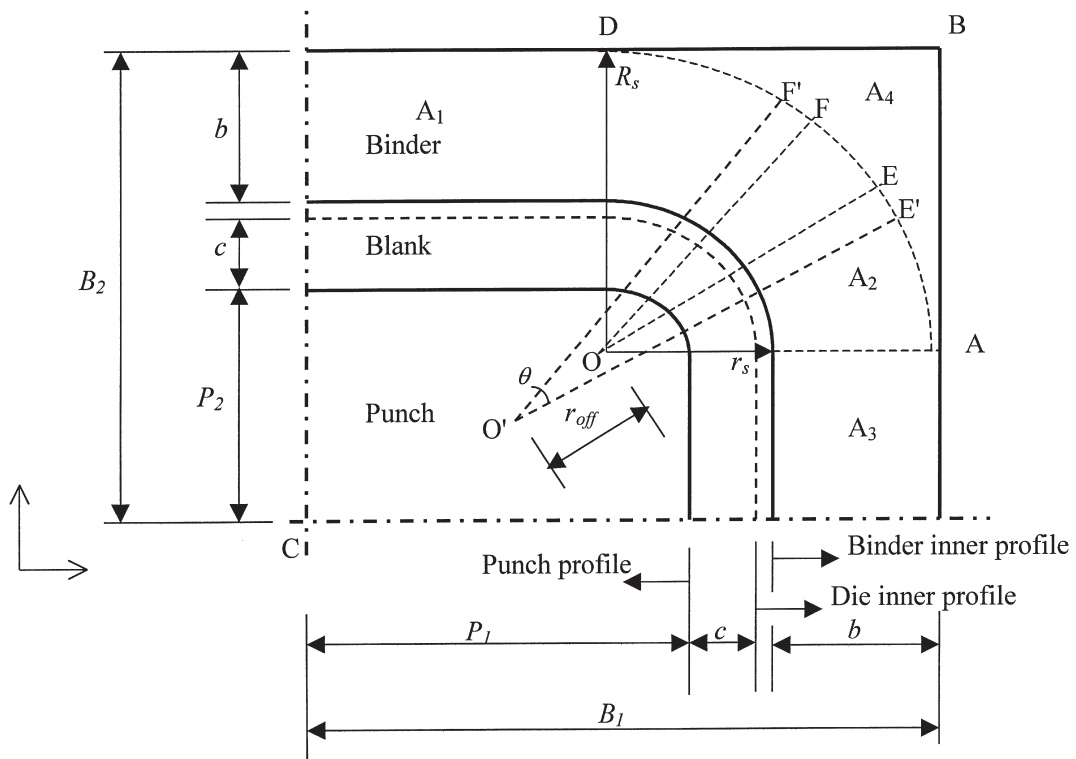


Fig. 1. Plan view of a quarter of a box and the simplified axisymmetric models with and without offset.

stretched into the corner section from under the punch and the material flowing toward the corner from the straight sides as the punch advances. Moreover, such a model cannot reflect the effects caused by varying the size and aspect ratios of the punch. Consequently, it provides conservative results, meaning that the corners can actually be formed deeper than predicted.

Here, we are proposing a new modeling methodology to address this issue, that is, adding a center offset to the axisymmetric model. Fig. 1 shows the axisymmetric model,  $O'E'F'$ , with a center offset  $r_{\text{off}}$ . The  $r_s$  and  $R_s$  are radii of the die opening and the blank size in the conventional axisymmetric model, respectively. The deformation of the extra material under the punch brought by the offset will delay the failure of the axisymmetric part. As a result, the 2D model with an adequate offset can reach the failure height of the 3D model and can be used to design the appropriate restraining force for the desired forming operation.

A successfully formed 3D part should have both the desired depth that is close to the failure height and the desired center strain to satisfy the geometry as well as the strength requirements. In the design of the rectangular cup forming process, the binder force to be used in the straight side can be found by using a 2D sectional analysis model according to both the desired center strain and the desired depth. To ensure the success of the forming process, a unique binder force needs to be applied at the corner such that the cup can be formed to the desired depth with the desired center strain  $\epsilon_C$ , which is the average of in-plane principal strains at point C in Fig. 1. Similarly, there is also an axisymmetric model with a unique offset that can be formed right to failure at the desired depth with a binder force equivalent to the binder force applied at the corner. Simulations as shown in the latter part of this paper verified that a relationship exists between the maximum center strain of the square cup and the center offset of the axisymmetric model. Systematically, this relation can also be formulated as follows.

In the 3D model, the binder force ( $F_b$ ) needed depends on the desired average in-plane center principal strain ( $\epsilon_C = (\epsilon_{1C} + \epsilon_{2C})/2$ ) of the 3D cup, the failure height ( $P_d$ ), material properties ( $m$ ), friction coefficient ( $\mu$ ) and the geometry of the tooling ( $g$ ). This can be expressed as:

$$F_b = f_1(\mu, g, m, P_d, \epsilon_C). \quad (1)$$

In the 2D axisymmetric model, the failure height ( $y_p^{2D}$ ) is decided by the center offset ( $r_{\text{off}}$  as shown in Fig. 1), the same  $m$ ,  $\mu$  and  $g$  as that of the 3D model, and the binder force ( $F_b^e$ ), which is equivalent to the restraining force per unit length along the die profile in the 3D model. This can be expressed as:

$$y_p^{2D} = f_2(r_{\text{off}}, m, \mu, g, F_b^e) \quad (2)$$

The failure height of the 2D axisymmetric model should match that of the 3D model. Therefore,<sup>1</sup>

$$P_d = y_p^{2D} \quad (3)$$

As mentioned above, the restraining force per unit length along the die profile should be the same in the 2D and 3D models. Therefore, the equivalent binder force obtained in the 2D model should be converted to the binder force used in the 3D forming process according to Eq. (4).

<sup>1</sup> Later in Section 5, we illustrated this relation should be  $y_p^{2D} = kP_d$ , where  $k$  is a function of tooling geometry. However, this will not affect the argument of uniqueness put forward in this section. Therefore, for simplicity, we use  $P_d = y_p^{2D}$  here.

$$F_b^c = \frac{F_b(A_2 + A_4)(r_{\text{off}} + r_s)\theta}{2\pi(A_1 + A_2 + A_3 + A_4)r_s} \quad (4)$$

where  $F_b$  is the total binder force applied in the 3D rectangular cup forming,  $A_1$ ,  $A_2$ ,  $A_3$  and  $A_4$  are the binder contact areas as shown in Fig. 1,  $r_s$  is the distance from the axisymmetric center O to the inner edge of the binder (Fig. 1) and  $\theta$  is the angle at the center of the axisymmetric model as shown in Fig. 1. When  $\theta=2\pi$ ,  $F_b^c$  is corresponding to the entire binder force applied in a full 2D axisymmetric cup forming.

With the above equations, the center strain of the 3D model can be related to the center offset in the 2D model. First, the  $y_p^{2D}$  in Eq. (2) can be replaced by  $P_d$  using Eq. (3). Then  $F_b^c$  in Eq. (2) can be replaced by  $F_b$  using Eq. (4). Finally, Eq. (1) can be substituted into Eq. (2) to eliminate  $F_b$ . The combination of the Eqs. (1)–(4) reveals that the center offset of the 2D model can be expressed as:

$$r_{\text{off}} = f(\mu, \epsilon_c, g, m, P_d) \quad (5)$$

This relationship indicates that the unique offset for the axisymmetric model can be obtained by using the desired center strain and the failure height of the 3D model. Since the center strain is obtained at the failure height, the optimized design must have been achieved. The function  $f$  in Eq. (5) is hereinafter referred to as the offset function. A detailed form of the function is given later in the paper.

### 3. Study of Numisheet'93 square cup

The square cup in Numisheet'93 [6] was studied to demonstrate the effectiveness of the proposed model. A variety of deep drawing tests with various binder forces and punch strokes were conducted. The experimental results provided very important information for detecting cup failure heights in the numerical simulations. By measuring the strains at the critical location below the punch radius at the corners, the unconventional forming limit diagram, which is based on the strain path in the forming process, was obtained. The obtained FLD<sub>0</sub> can then be used as a criterion to detect necking in the numerical models. Since cup failure heights obtained from the numerical simulations match experimental results very well, the failure criterion and our numerical models are proven to be reliable and accurate. Therefore, failure heights in this research can be found numerically without further experiments.

#### 3.1. Experiments of cup forming

The geometry of the tooling is the same as the Numisheet'93 benchmark test as shown in [6]. Experiments were conducted in a MTS Formability System, Model 866.11Q-A2, with a clamping capacity of 2000 kN, a punch capacity of 1000 kN, and a maximum punch stroke of 225 mm. The material used in the experiments was mild steel (AKDQ), with a thickness of 0.796 mm, Young's modulus of 206 GPa, Poisson's ratio of 0.3 and average  $R$ -value of 1.705. The tensile properties of the material are given in Table 1. The friction coefficient was measured as 0.1 by a draw bead simulator. (The lubricant used in the experiment was Ferrocok 61A US.) Blanks

Table 1  
Tensile properties of the test material

Angular offset from rolling direction (degree)	Yield stress (MPa)	Ultimate tensile stress (MPa)	<i>n</i> Value	<i>K</i> (MPa)
0	174.2	314.7	0.207	537.4
45	174.8	324.8	0.199	547.4
90	197.4	310.7	0.198	523.2
Mean	$\sigma = 540.6 \epsilon^{0.2037}$ (MPa)			

were sheared to a size of 150 mm×150 mm, and a 2 mm circle grid pattern was applied for measuring strains. Parts were then formed with a punch speed of 10 mm/second. Care was taken to assure that the part was symmetrically aligned with respect to the punch and binder, and the rolling direction was oriented consistently in the tooling. The maximum forming depth for the experiments was set at 43.5 mm. Binder force was varied in the experiments to the following values: 19.6, 40, 60, 70, 80, 90, 100, 120, 160, 200, and 240 kN. For binder forces less than 90 kN, the full punch stroke of 43.5 mm was completed without tearing failure in the parts. Buckling in the side wall of the parts occurred for binder forces less than 70 kN. To determine the maximum forming depth before necking failure occurred for parts with a binder force greater than 100 kN, samples were run with different punch strokes to induce tearing failure in the parts. These forming depths assured that tearing failure would occur for all of the binder force values in at least one corner of the samples. Engineering strains were then measured from the circle grid pattern and were converted to true strain for comparison with simulation results. Efforts were also made to find the punch stroke just prior to failure, i.e. just as splitting was beginning to occur. More tests were then conducted around that forming height to catch the critical strains before and after tearing failure occurs. Thus, more strain points close to the forming limit curve were obtained.

### 3.2. Experimental results

During the experiments, punch force was recorded along with punch displacement. Fig. 2 shows the punch force trajectory for the binder force case of 100 kN. Necking was considered to occur as the binder force reached its maximum value and started to drop. Following necking, splitting occurred at the point of the large drop in the punch force. Using this criterion, punch displacements where necking and splitting occurred for all the binder forces used in the test were obtained. Table 2 shows the average necking and splitting heights for the Numisheet'93 geometry.

Another important measurement from the experiments was the strains at the critical location in the formed cups. The strains were obtained by measuring the circle grids at the punch radius. Most failures occurred at or above the corner point tangent to where the blank separated from the punch nose. Major and minor strains at both the necking or splitting corners and the non-failure corners were measured. Due to the symmetry of the cup, the strains at the non-failure corner are quite close to those at necking. Fig. 3 shows the collection of measured critical true strains. The solid line dividing the failure and non-failure points represents the left side of the forming limit diagram of the material. Notice that this obtained Forming Limit Curve (FLC) might be different from the standard FLC for this material due to the nonlinearity of strain paths involved

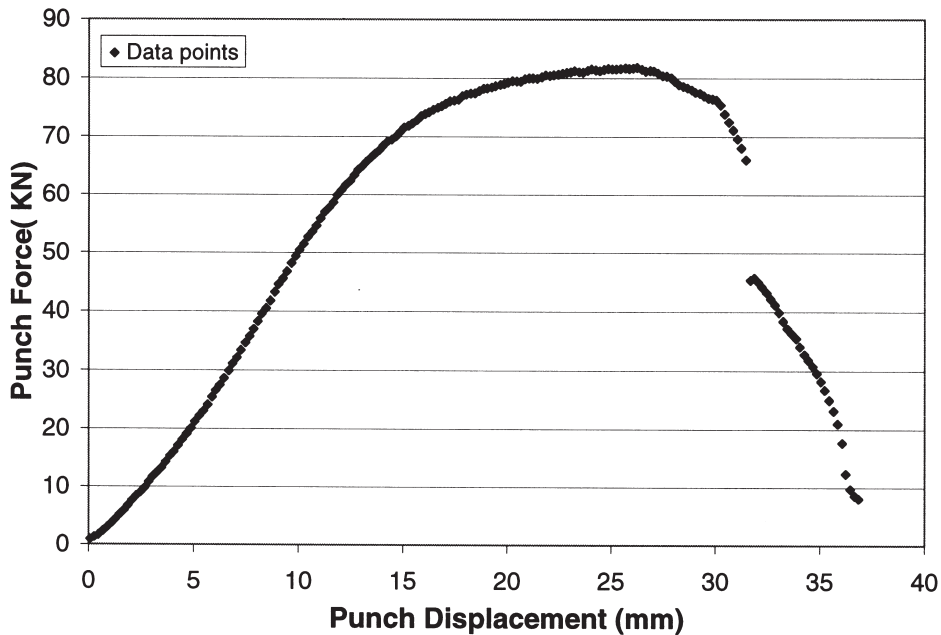


Fig. 2. Punch force trajectory for the 100 kN binder force case in the forming of the Numisheet'93 cup.

Table 2

Average forming heights of the Numisheet'93 square cup

Binder force (kN)	100	120	160	200	240	280
Splitting depth (mm)	30.95	27.16	21.45	17.94	16.90	16.80
Necking depth (mm)	26.58	23.84	20.43	17.52	16.57	16.42

in this test. This plot shows the failure strain levels in the plane strain condition ( $FLD_0=0.3$ ) and those on the left-hand side of the forming limit diagram. This  $FLD_0$  was used for determining necking in the simulations and proved to be a very accurate failure criterion as demonstrated in the following section.

### 3.3. Numerical simulation

#### 3.3.1. Finite element model

To find the offset function,  $f$ , in Eq. (5), the finite element model of the above square cup forming was created and the numerical results were compared with the experimental results. The deformed mesh of the finite element model is shown in Fig. 4. A quarter of the square cup is modeled to take advantage of the symmetric conditions. Proper symmetric boundary conditions were applied. A commercial explicit three-dimensional finite element program LS-DYNA3D [7] was used for the simulation. The elements used were 4-node Belytschko–Tsay shell elements, which provide five integration points through the thickness of the sheet metal. This element

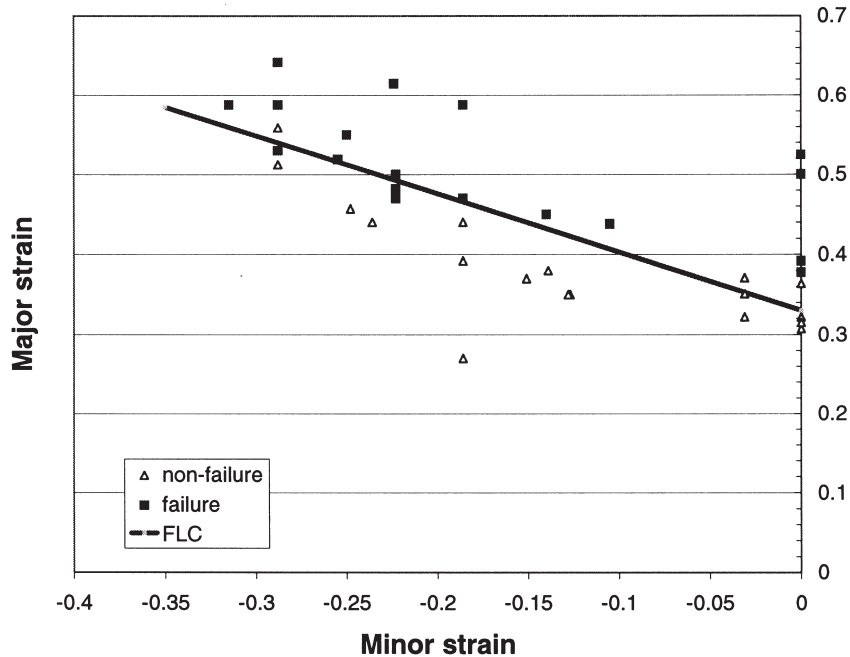


Fig. 3. Measured distribution of critical strains from Numisheet'93 square cup forming tests and the Forming Limit Curve (FLC).

accounts for both the stretching and bending incurred in the sheet. The tooling was modeled as rigid surfaces. A Coulomb friction law was employed to account for the frictional force with a friction coefficient of 0.1, the same as that measured in the experiment. The material was assumed to be transverse anisotropic (isotropic in the plane of the sheet metal) with isotropic strain hardening. The yielding of the material was modeled by Barlat's yield function [8], which can be expressed as:

$$\Phi = a|K_1 + K_2|^k + a|K_1 - K_2|^k + c|2K_2|^k = 2\bar{\sigma}^k \quad (6)$$

where  $k=6$  is used for mild steel, and  $\bar{\sigma}$  is the equivalent yield stress. The detailed definition of coefficients  $a$ ,  $c$  and stress combination  $K_{i=1,2}$  are given in [7,8].

### 3.3.2. Verifications of the numerical model

The numerical model with Barlat's yield function was first verified by using material properties of the mild steel specified in Numisheet'93 [6]. The thickness strain distributions of the deformed cup were compared with the experimental data reported in [6] as shown in Fig. 5. The thickness distribution of the deformed cup was also compared with the results obtained by using Hill's 1948 yield criterion. The results show that using Barlat's yield criterion with the exponent  $k$  value equal to 6 agrees with the localization of the deformation better than using Hill's 1948 yield criterion. Overall, very good agreement between experiments and simulations using Barlat's yield criterion was obtained.

Fig. 6 shows the plot of major strains versus punch displacements for a few elements along

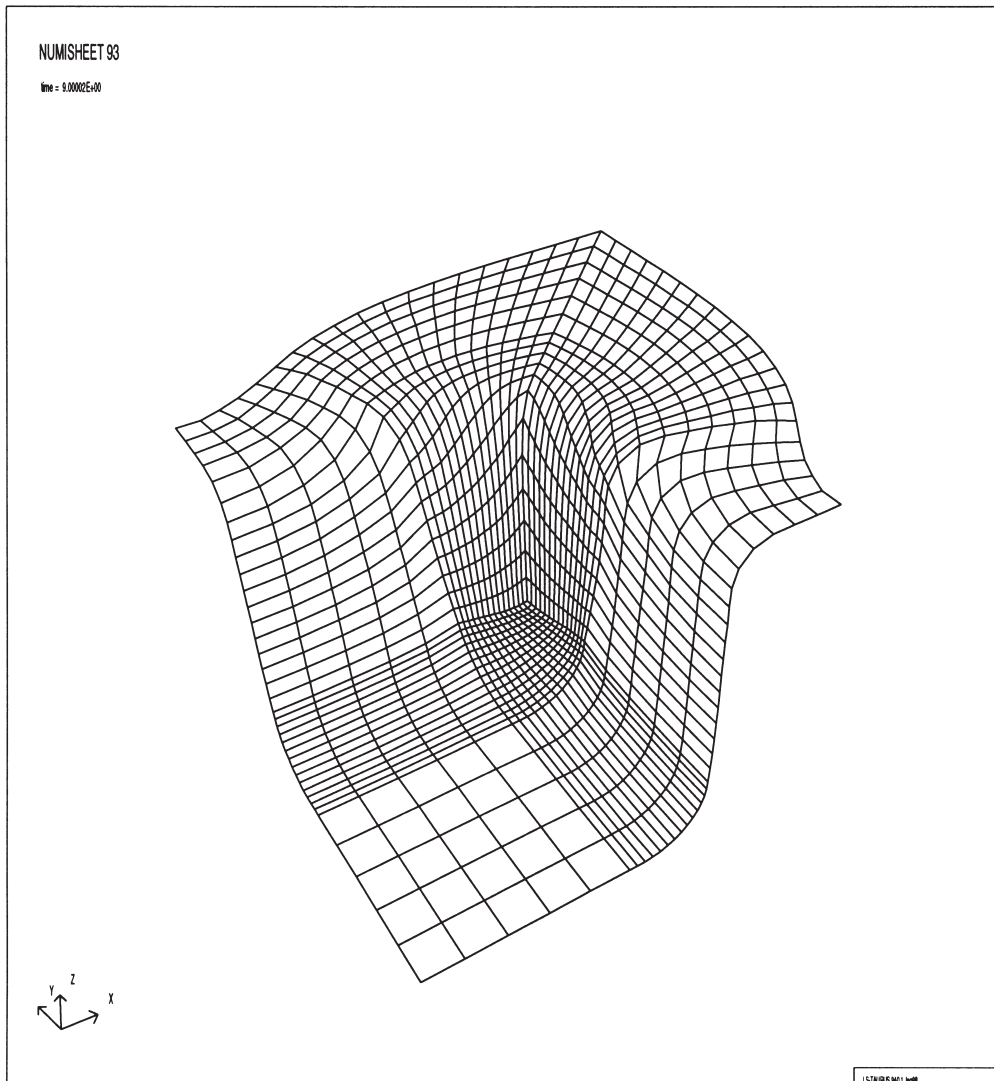


Fig. 4. Deformed finite element mesh of the square cup forming.

the radial direction at the critical punch nose area. Cup failure in the simulation was identified to be the dramatic increase in the deformation of one element. Obviously, the principal strain of element No. 346 is blowing up while strains of the other elements are leveling off. Necking is considered to have occurred when the maximum principal strain of element 346 reaches the  $FLD_0$ , which is 0.3 as determined by the forming limit diagram obtained in the experiments. By using this method, the failure heights of the cups were determined and compared with the experimental data as shown in Fig. 7. Excellent agreement was achieved. The numerical model and the failure criterion are therefore validated by the experimental data.

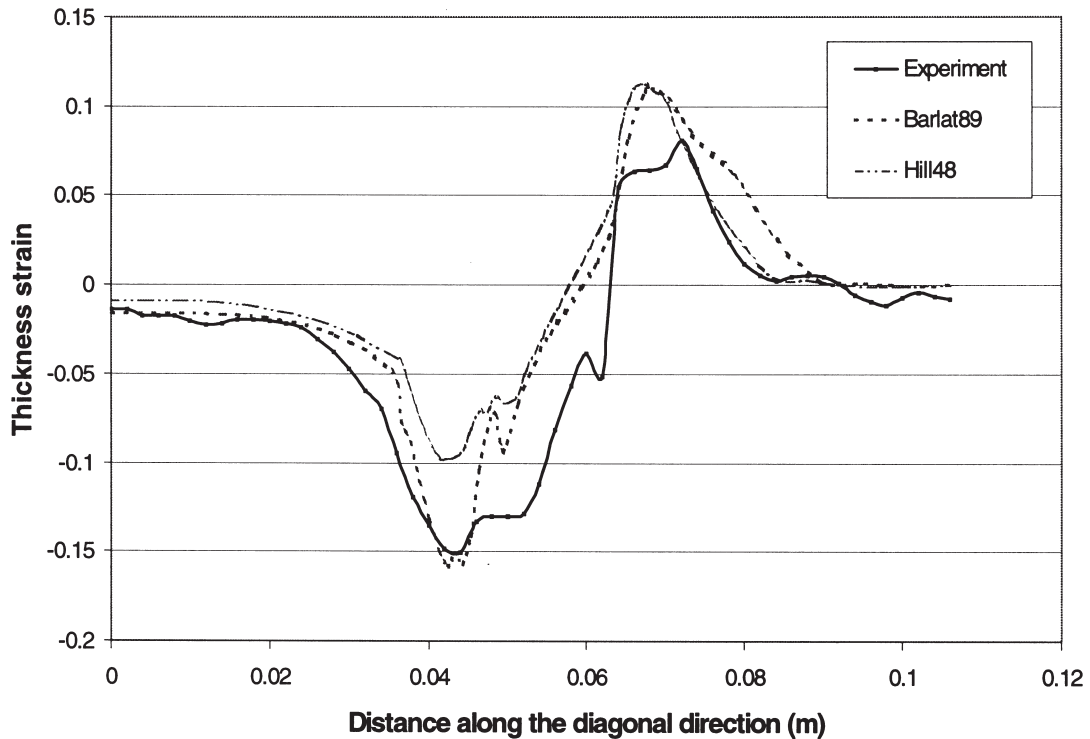


Fig. 5. Comparison of the thickness strain distribution along the diagonal path.

#### 4. Finding the center offset

With confidence in our numerical model and failure criterion, the modified axisymmetric model with a center offset as proposed in Section 2 was built to match the failure height in the 3D model. By adding the offset, the blank size and the punch size as well as the binder size were increased by a specific amount. The binder force in the 2D model was changed according to Eq. (4). However, the clearance between the punch and the binder was not affected. Finally, by matching the failure heights, a unique offset can be found for a certain cup forming case.

#### 5. Effect of tooling/process parameters on offset

Following the study of the Numisheet'93 model, the effects of tooling/process parameters on the offset were examined. A number of deep drawing simulations were conducted for square cups with variations in material, friction and tooling geometry. The offset was found to be a function of center strain, forming depth, and the tooling/process parameters.

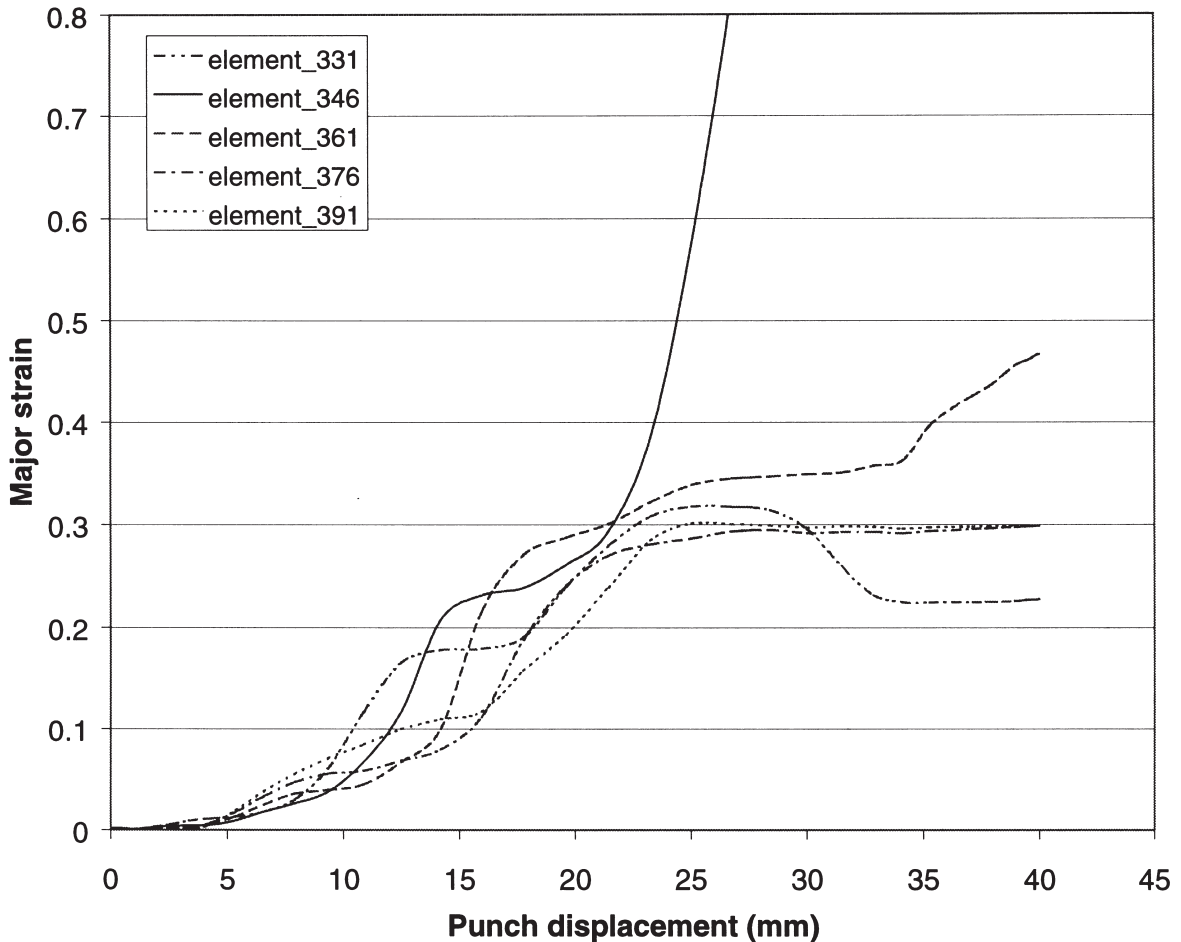


Fig. 6. Strain histories of the critical area elements in the square cup simulation with a binder force of 160 kN and a friction coefficient of 0.1.

### 5.1. Cases examined

The basic model for this study was the Numisheet'93 square cup. A number of 3D models were simulated with various combinations of geometry, material properties and friction coefficients. For each combination, binder forces, ranging from one that barely caused the cup to split to one beyond which the failure height was leveling off, were applied in the simulations. Matching the failure heights of the 2D and 3D models, offsets for the 2D axisymmetric models were also found by trial and error. Using the data from different models described below, we generated the function reflecting the relationships between the offset and variables such as center strain, friction coefficient,  $FLD_0$  of the material and geometric parameters of the tooling in Section 5.2.

Geometry variations studied in this paper include scaling up the entire Numisheet'93 model to 5 or 10 times the original size and increasing the punch–die clearance by 5 to 10 times the initial value. The thickness of the blank was kept constant. When the model size was scaled up, both

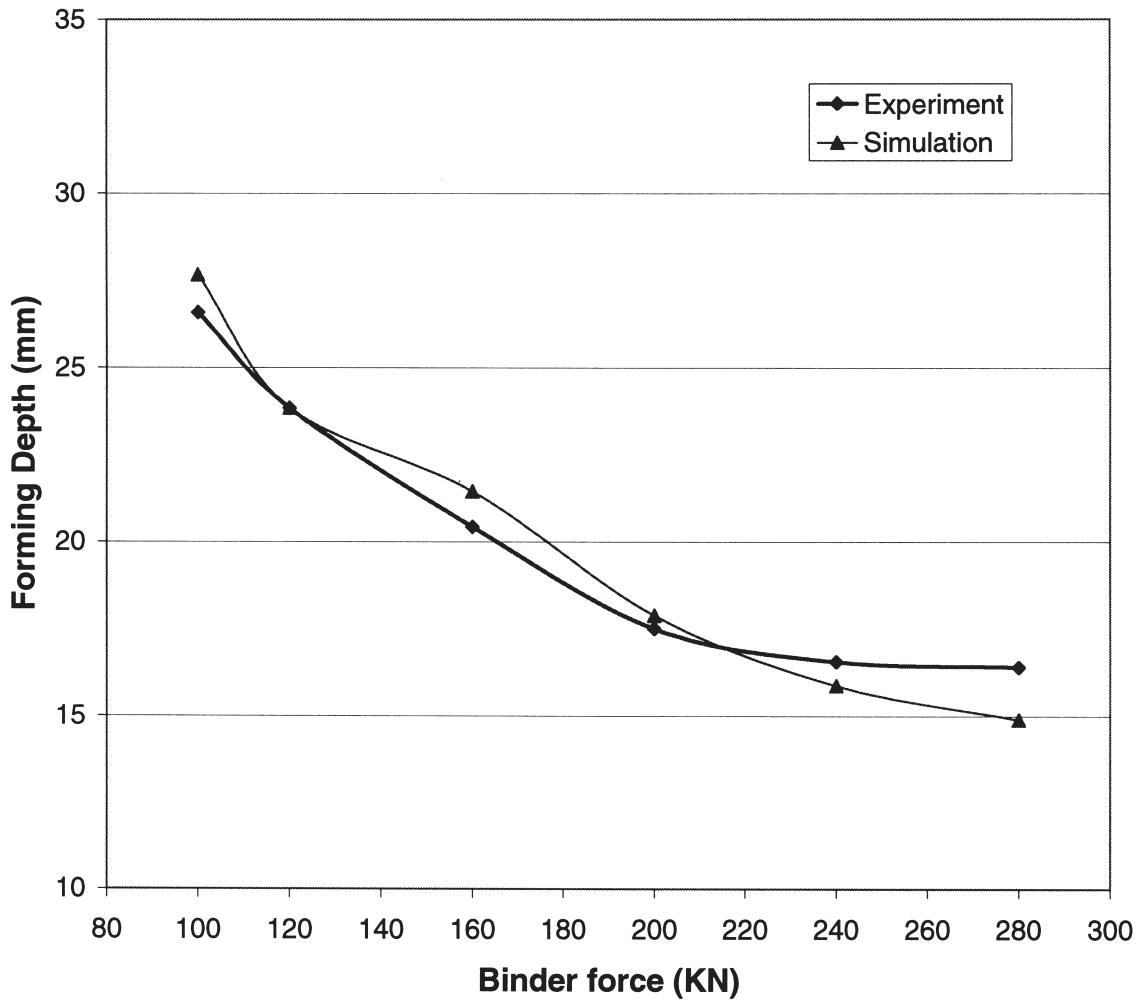


Fig. 7. Failure height diagram of the Numisheet'93 cup obtained from experiments and simulations.

the center strain and the failure height were increased. When increasing the punch–die clearance, the punch size was unchanged while the blank and binder sizes were increased by an equal amount. Increasing the clearance is in effect increasing the amount of material in the draw wall area. As a result, the failure height was increased without significant change to the center strain. Finally, the variations of the size and aspect ratios of the punch were studied. Changing the punch size and aspect ratio is in fact changing the draw ratio,  $d$ , of the model, which is defined in this paper as:

$$d = \frac{1}{2} \left( \frac{B_1}{P_1} + \frac{B_2}{P_2} \right) \quad (7)$$

where  $P_1$ ,  $P_2$ ,  $B_1$  and  $B_2$  are illustrated in Fig. 1.

Friction coefficients of 0.06, 0.1 and 0.15 were used in the simulation. As friction force

Table 3  
Simulations of square cup forming<sup>c</sup>

Case No. <sup>a</sup>	Material <sup>d</sup>	FLD <sub>0</sub>	$\mu$	$P_1 \times P_2$ (mm) <sup>b</sup>	$B_1 \times B_2$ (mm) <sup>b</sup>	$c$ (mm) <sup>b</sup>
AKDQ_f10_s1c11	AKDQ	0.3	0.10	35×35	75×75	2
AKDQ_f10_s5c11	AKDQ	0.3	0.10	175×175	375×375	10
AKDQ_f10_s10c11	AKDQ	0.3	0.10	350×350	750×750	20
AKDQ_f10_s5c15	AKDQ	0.3	0.10	175×175	415×415	50
AKDQ_f10_s5c110	AKDQ	0.3	0.10	175×175	415×415	50
AKDQ_f15_s5c15	AKDQ	0.3	0.15	175×175	415×415	50
AKDQ_f06_s5c15	AKDQ	0.3	0.06	175×175	415×415	50
A180DR_f10_s5c15	A180DR	0.3	0.10	175×175	415×415	50
AA6111_f10_s5c15	AA6111	0.223	0.10	175×175	415×415	50

<sup>a</sup> The geometry of case AKDQ\_f10\_s1c11 is the square cup of Numisheet'93 model.

<sup>b</sup> The  $P_1$ ,  $P_2$ ,  $B_1$ ,  $B_2$  and  $c$  are illustrated in Fig. 1.

<sup>c</sup> The thickness of the blank is kept at 0.796 mm in all the models.

<sup>d</sup> Material types: A180DR—High strength steel; AA6111—Aluminum AL6111-T4; AKDQ—Mild steel.

decreases, the failure height and the corresponding center strain increase due to more stretching of the material under the punch. Therefore, the influence of the friction coefficient must be taken into account.

Various materials of steel and aluminum were used in the simulation. Although these materials have various  $K$ ,  $n$  and  $R$  values, the most significant difference is their FLD<sub>0</sub> which directly determines the failure height of the square cup. Summaries of these models are listed in Tables 3 and 4.

## 5.2. Offset function and its verification

The results obtained from the above simulations for square cups in Table 3 are summarized in Fig. 8, where offset is plotted against the center strain in the 3D cup. The labels of the curves correspond to the case numbers in Table 3. Each data point represents one simulation with one

Table 4  
Simulations of square and rectangular cup forming

Case number	Material	FLD <sub>0</sub>	$\mu$	$P_1 \times P_2$ (mm)	$B_1 \times B_2$ (mm)	$c$ (mm)
S1c15_1_1_1	AKDQ	0.3	0.10	60×60	108×108	10
S1c11_0.5_1_1	AKDQ	0.3	0.10	60×35	100×75	2
S1c11_0.5_1_1.5	AKDQ	0.3	0.10	85×35	125×75	2
S1c15_1_1_2	AKDQ	0.3	0.10	110×60	158×108	10
S5c15_1_1_1	AKDQ	0.3	0.10	300×300	540×540	50
S5c15_1_1_2	AKDQ	0.3	0.10	550×300	790×665	50
S5c11_0.5_1_1	AKDQ	0.3	0.10	300×175	500×375	10
S1c15_2_1_3	AKDQ	0.3	0.10	160×110	208×158	10

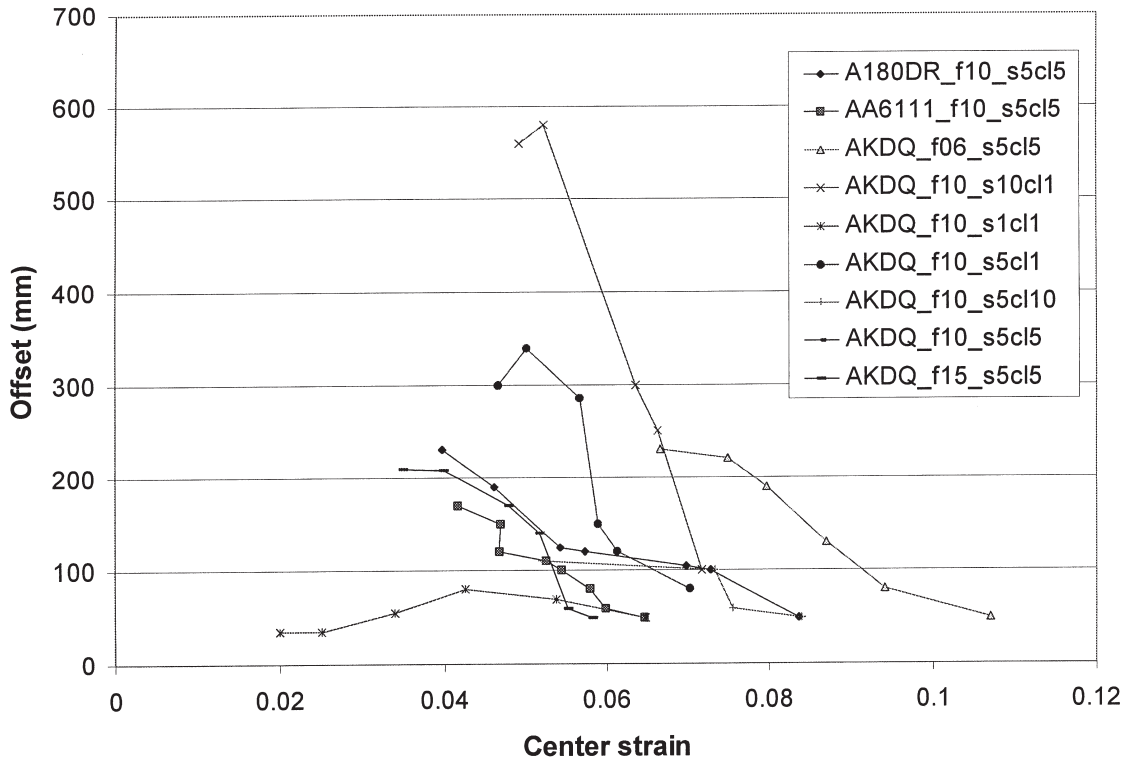


Fig. 8. Center offset versus center strain for square cups listed in Table 3.

binder force. Obviously, there is a trend that the offset is decreasing when the center strain is increasing.

For the cases in Table 4, a change in the draw ratio is created due to variations in the punch dimensions  $P_1$  and  $P_2$  (Fig. 1). The punch displacement,  $P_d$ , increases with the decrease of the draw ratio,  $d$ . Therefore in this work, a draw ratio factor  $k$  and a reduced failure height,  $y_p^{2D}$ , are introduced to maintain the trend between offset versus center strain as shown in Fig. 8 and they are defined by

$$k = \frac{d_1 d_2}{d_0 d} \quad (8)$$

and

$$y_p^{2D} = k P_d \quad (9)$$

where  $d_0 = B_0/P_0$ ,  $d_1 = B_1/P_1$ , and  $d_2 = B_2/P_2$ . For the special case, when the change of the draw ratio is only caused by clearance variation while  $b/P = b_0/P_0$ ,  $k$  is equal to 1. (In Numisheet'93 model,  $P_0 = 35$  (mm),  $B_0 = 75$  (mm) and  $b_0 = 33$  (mm), and  $b$  is illustrated in Fig. 1.) The idea is to locate the offset of a 2D model that is able to reach the modified failure height  $y_p^{2D}$ . The located offsets

are plotted versus the center strain as shown in Fig. 9. Again, the same trend as seen in Fig. 8, decreasing offset with increasing center strain is observed.

Even though the offsets are basically inversely proportional to the center strains as shown in Figs. 8 and 9, no rules can be concluded without normalizing the offsets and failure heights by the geometric size and other geometric parameters such as clearance and punch size etc. After some trial and error, the normalized curve (shown in Fig. 10) for the offset was found. The normalization makes it possible to fit the originally scattered data into a curve and find the law governing the physics. The curve fitting for the relations of offset versus center strain is plotted as the solid line in Fig. 10. With some mathematical manipulation, the offset reference curve can be expressed as:

$$r_{\text{off}} = \frac{0.358\text{FLD}_0^{2.1286}k^{1.3853}}{\epsilon_c^{1.4106}p^{4.2318}y_p^{0.4334}C_p^{0.6411}\mu^{1.0643}} \quad (10)$$

In addition to those defined before, some additional variables in Eq. (10) are defined as the following with reference to Fig. 1:

1. To normalize the offset and failure height, the geometric size of the model,  $S$ , is defined as:

$$S = k \frac{B}{B_0} \quad (11)$$

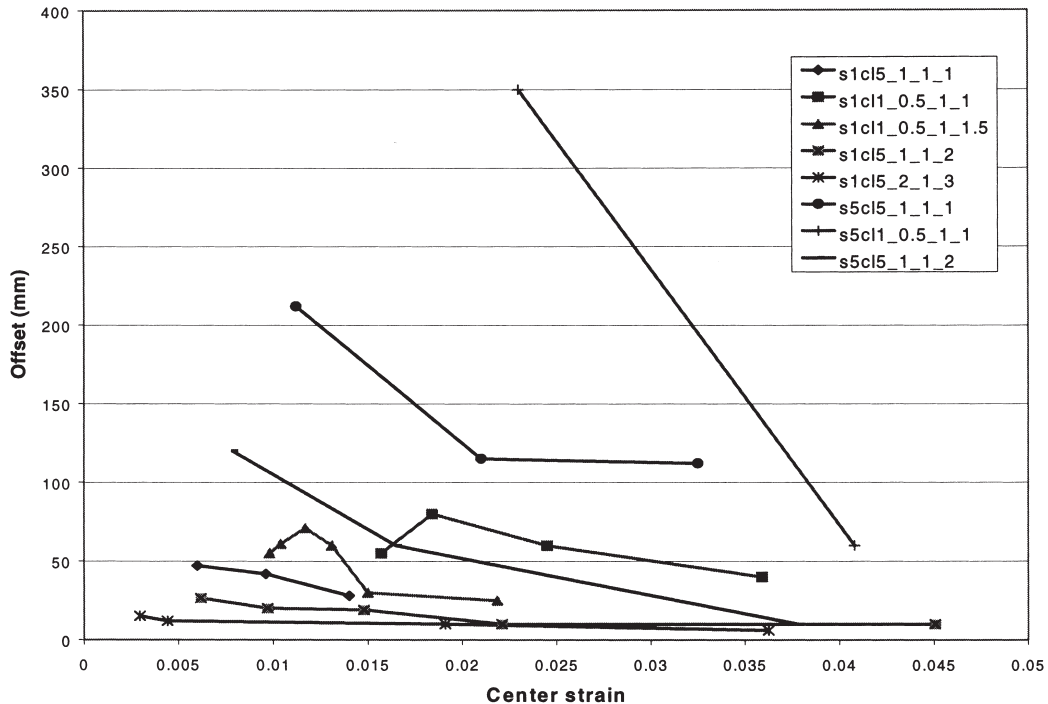


Fig. 9. Center offset for the normalized failure height versus center strain for square and rectangular cups listed in Table 4.

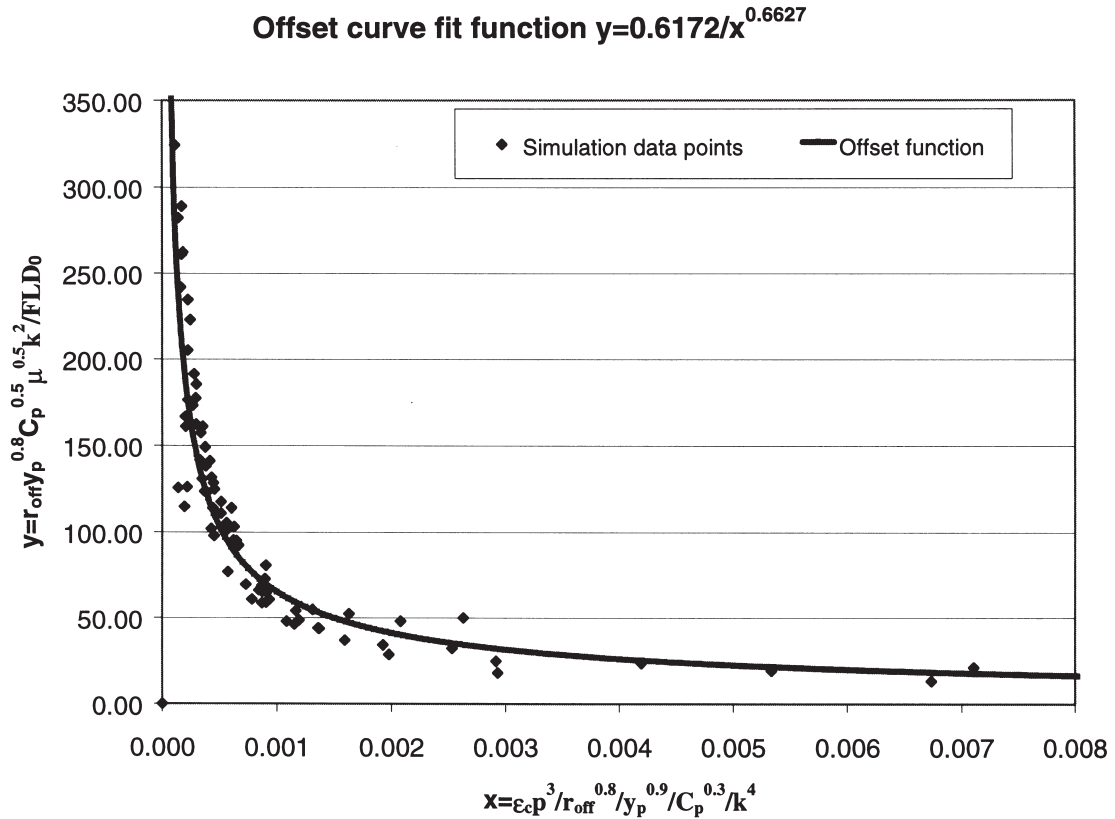


Fig. 10. Normalized curve for offset versus center strain.

2. The center offset  $r_{\text{off}}$  (mm) is normalized by the geometric size of the model,  $r_{\text{off}} = r_{\text{off}}^{2D} / S$ , where  $r_{\text{off}}^{2D}$  is the offset used in the 2D model and  $S$  is the geometric size.
3. The center strain  $\epsilon_C$  is the averaged center strain, i.e.  $\epsilon_C = (\epsilon_{1C} + \epsilon_{2C}) / 2$ , where  $\epsilon_{1C}$  and  $\epsilon_{2C}$  are the in-plane principal strains at the center of the cup (point C in Fig. 1).
4.  $C_p$  is the ratio of the clearance to the punch size, i.e.  $C_p = c / P$ , where  $P$  is the averaged punch size, i.e.  $P = (P_1 + P_2) / 2$ .
5.  $y_p$  is the normalized punch displacement. If  $P_d$  represents the actual failure height of the 3D model, then  $y_p = (P_d / S) k$ .
6.  $p$  is the normalized punch size ratio, i.e.  $p = P / (P_0 S)$ .
7.  $\mu$  is the friction coefficient.

The offset function reflects the physics of the deformation in the deep drawing process. Generally, with the increase of  $FLD_0$  and decrease of friction, the forming depth increases and more material flow-in occurs. As a result, the offset increases with  $FLD_0$  and is inversely proportional to the friction coefficient. The punch displacement and the center strain are related to each other. When the binder force is large, the punch displacement will be small, and therefore the center

strain is large. Hence, the offset will drop when the center strain is increased. The function also indicates that the clearance, punch size and draw ratio play important roles in the deformation. Finally, the form of the offset function is independent of the size of the model since both the offsets and punch displacements were normalized. In addition, Eq. (10) is found to be suitable for cases where corner radii of the tooling have been changed. In fact, the change of the tooling corner radius implicitly affects the center strain.

To investigate the accuracy of the offset function, 2D models with the offsets obtained from Eq. (10) were simulated. The predicted failure heights were then compared with the failure heights obtained from the 3D models. As seen from Fig. 11 showing the error distribution for predicted failure heights, very good agreement is achieved. We have a 44% chance that our error of failure height prediction is within 10% and nearly a 80% chance of having less than 20% error. Only in a few cases were the errors above 30%. These were the cases when the cup barely reaches failure under a low binder force. In these cases, a small inaccuracy of the predicted offset can lead to a false non-failure result. Therefore, special care needs to be taken when low binder forces are used to reach deep forming heights with small center strains. The punch sizes used in the simulations range from 70×70 mm to 1100×600 mm. The average error of the predicted failure height was 14.8% compared to 45.6% when no offset was used. The 2D models with offsets have made significant improvements in predicting the corner failure heights of 3D cups.

### 6. Design algorithm

The offset function can be used in designing the corner part of the square and rectangular cups. For any given geometry, friction coefficient, material properties and desired center strain

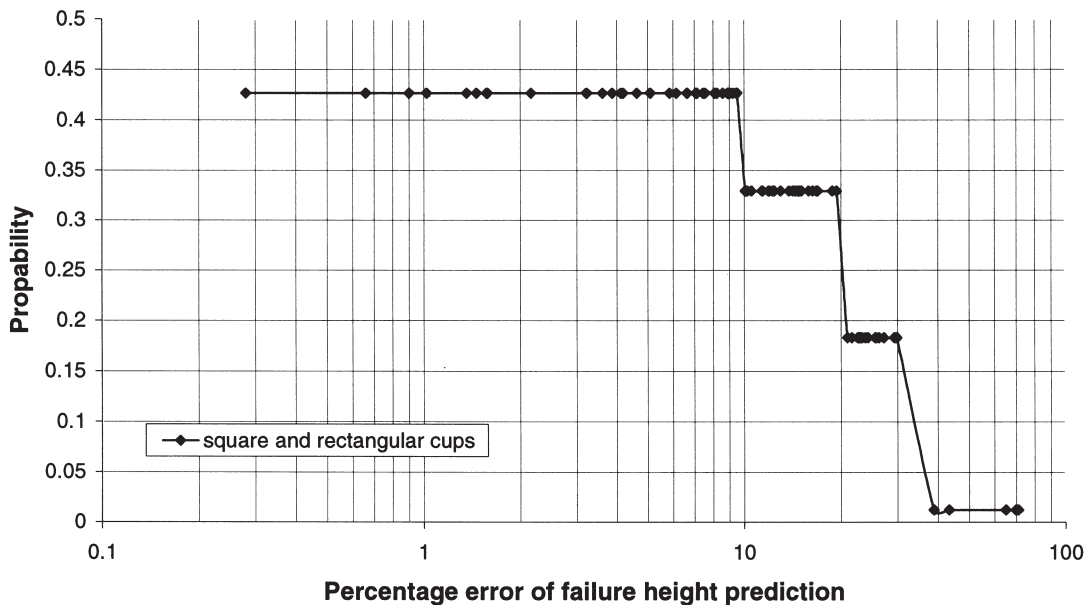


Fig. 11. Absolute error distribution of the failure height prediction.

requirements, the binder force can be easily designed by using the 2D axisymmetric models with the center offset obtained from Eq. (10). If the obtained binder force is unrealistic, then changes of geometry or any other tooling/process parameters can be made. The design procedure for a corner part is as follows:

1. Calculate the geometric size and other normalized parameters,  $k$ ,  $S$ ,  $p$ , and  $C_p$  as defined in Section 5.
2. Normalize the desired cup forming depth  $P_d$  by the size  $S$  and draw ratio factor  $k$ . The punch displacement to be used in the offset function can be obtained as  $y_p=(P_d/S)k$ .
3. Obtain the information of desired center strains  $\epsilon_{C1}$  and  $\epsilon_{C2}$  corresponding to the requirements of the part and the values of  $FLD_0$  and the friction coefficient  $\mu$ .
4. Use Eq. (10) to calculate the normalized offset  $r_{off}$ . The offset to be used in the 2D model is  $r_{off}^{2D}=r_{off}S$ .
5. Build a 2D axisymmetric model according to the corner geometry of the part and the calculated offset  $r_{off}^{2D}$ .
6. Run the 2D model with various binder forces until the forming depth  $y_p^{2D}$  is obtained, where  $y_p^{2D}=P_d k=y_p S$ . Notice that this 2D axisymmetric problem can be solved by the Finite Element Method or by analytical solution. The second approach will further improve the ability of rapidly assessing the manufacturability.
7. Use Eq. (4) to calculate the binder force ( $F_b$ ) to be used in the 3D forming, which can be converted according to the ratio of the contact area at the corner ( $A_2+A_4$ ) to the complete binder contact area ( $A_1+A_2+A_3+A_4$ ).

The above design algorithm is being incorporated into the design process used by the manufacturing team of General Motors.

## 7. Conclusion and future work

This work has provided a simplified 2D axisymmetric model with a center offset to efficiently determine the binder force required for a projected 3D deep drawing process. A relationship exists between the center strain of the cup and the center offset of the axisymmetric model. Through curve fitting of the data from the simulations, the offset of the 2D model is found to be a function of the geometry of the tooling, material properties, friction conditions and center strain requirement of the desired 3D cup. The average error of predicted failure height using a 2D axisymmetric model with the proposed offset was reduced from 45% to 15% compared to models with no offset. An algorithm is proposed to design the restraining force used in an actual forming process. The proposed model provides the designer with a powerful tool to rapidly assess the manufacturability of the desired part. This method will be extremely valuable at the early design stage of sheet metal parts.

Future work will concentrate on geometric variations, including variations of the corner plan view radius  $r_s$  in Fig. 1, blank thickness and punch shape. The offset function and design algorithm will be improved and verified in the design and simulation of the forming process for complicated stamping panels.

## Acknowledgements

The authors would like to express appreciation to General Motors for their financial support, to National Steel, in particular, Dr David Meuleman for assistance with the experimental work, and Dr Mahmoud Demeri of the Ford Research Lab for providing us with the Numisheet'93 tooling.

## References

- [1] Ing Eckart Doege, Prediction of failure in deep drawing. Proceedings of the 12th Automotive Materials Symposium, 1985.
- [2] M.J. Saran, Y.T. Keum, R.H. Wagoner, Section analysis with irregular tools and arbitrary draw-in conditions for numerical simulation of sheet forming, *Int. J. Mech. Sci.* 33 (11) (1991) 893–909.
- [3] A. Brooks, R. Jhita, C.M. Ni, Applications of a two-dimensional metal forming analysis tool to production stamping problems, *SAE Transactions* 100 (5) (1991) 751–758.
- [4] T. Walker, J. Kolodziejski, M. Karima, Using axisymmetric solutions to estimate the forming severity of three dimensional metal stampings. SAE Paper 920636, *Autobody Stamping Applications and Analysis*, SAE SP-897, 1992, pp. 161–172.
- [5] C. Wong, R.H. Wagoner, M.L. Wenner, Corner design in deep drawn rectangular parts. SAE Paper 970437, 1997, pp. 39–55.
- [6] A. Makinouchi, E. Nakamachi, E. Onate, R.H. Wagoner, Numerical simulation of 3-D sheet metal forming processes verification of simulation with experiment. Proceedings of the 2nd International Conference Numisheet'93, 1993.
- [7] LS-DYNA3D User's Manual, Version 940, 1997.
- [8] F. Barlat, J. Lian, Plastic behavior and stretchability of sheet metals. Part I: A yield function for orthotropic sheets under plane stress conditions, *Int. J. of Plast.* 5 (1989) 51–61.